Please cite the Published Version

Covert Communication in Downlink NOMA Systems with Channel Uncertainty

Yanliang Zhang, Wenjing He, Xingwang Li, *Senior Member, IEEE,* Hongxing Peng, Khaled Rabie, *Senior Member, IEEE,* Galymzhan Nauryzbayev, *Senior Member, IEEE,* Basem M. ElHalawany, *Senior Member, IEEE* and Mingfu Zhu

Abstract—With the gradual promotion of the fifth generation mobile communication and Internet of Things (IoT) applications, wireless communication transmission will be more vulnerable to illegal interceptions and/or attacks. To ensure communication security, we study covert communication of downlink non-orthogonal multiple access (NOMA) systems, where the channel knowledge of users is uncertain. A multi-antenna transmitter tries to covertly transmit information to a covert user (strong user) through the shield of a public communication link (weak user), while the warden tries to detect the communication behavior between the transmitter and covert user. To improve security and energy efficiency, the k-th best antenna of the transmitter is selected, since the optimal antenna may be not available due to some schedule and/or other reasons. Aiming to evaluate the proposed framework performance, we start by deriving exact expressions for the minimum detection error probability and the optimal detection threshold of the warden, followed by a calculation analysis of the expected minimum detection error probability and the outage probability of NOMA users. The asymptotic behavior for the outage probability is investigated at high signal-to-noise ratio in order to acquire greater useful insights. With the goal of improving the system covertness performance, we propose that a scheme is optimized to enhance the covert throughput of the system to the maximum. Simulation results show that: 1) channel estimation errors have a significant effect on system performance; 2) reliability performance tends to build up as the total number of antennas grows large; 3) as the transmitting power and number of antennas increases, there is an upper bound for maximizing the covert throughput.

Index Terms—Covert communication, channel estimation errors, expected minimum detection error probability, NOMA

Yanliang Zhang, Wenjing He, Xingwang Li and Hongxing Peng are with the School of Physics and Electronic Information Engineering, Henan Polytechnic University, Jiaozuo 454000, China (email: Ylzhang@hpu.edu.cn, hewenjing07@163.com, lixingwangbupt@gmail.com, phx@hpu.edu.cn).

Khaled Rabie is with the Department of Engineering, Manchester Metropolitan University, Manchester M1 5GD, U.K. (e-mail: k.rabie@mmu.ac.uk).

Galymzhan Nauryzbayev is with the Department of Electrical and Computer Engineering, School of Engineering and Digital Sciences, Nazarbayev University, Nur-Sultan 010000, Kazakhstan (e-mail: galymzhan.nauryzbayev@nu.edu.kz).

Basem M. ElHalawany is with Benha University, Cairo 11672, Egypt (e-mail: basem.mamdoh@feng.bu.edu.eg).

Mingfu Zhu is The College of Computer Science and Technology, Henan Polytechnic University, Jiaozuo 454003, China (e-mail:zhumingfu@zzu.edu.cn).

I. INTRODUCTION

With the speedy development towards the mobile Internet, social networks and Internet of Things (IoT), mobile smart terminals are becoming increasingly popular, and the explosive growth of mobile data services is putting more and more demands on wireless communication systems [1]. In parallel, the exponentially growing data traffic poses an enormous challenge to the restricted spectrum resources [2, 3]. Therefore, non-orthogonal multiple access (NOMA), which can support large-scale connections, higher spectrum efficiency and energy efficiency, has become a research hotspot for the industry 4.0 and academia [4]. NOMA meets not only the needs of fifth generation (5G) with respect to the spectrum efficiency and number of connections, but also the heterogeneous needs of low latency, high reliability, improved fairness and high throughput [5, 6]. In contrast to the orthogonal multiple access (OMA) technology, NOMA achieves multiplexing of the power domain (PD) for the users [7–10]. Consequently, it is possible for users in the NOMA system to transmit or receive data on the same resources block of time and frequency. The core of NOMA technology is the provision of multi-user services through superposition coding (SC) at transmitters and successive interference cancellation (SIC) at receivers [11, 12]. As a result, NOMA not only improves spectrum utilization, but also addresses the issue of fairness of user communications.

NOMA has already drawn the wide attention of researchers in the field of wireless communications [13–20]. In the downlink NOMA networks, Sindhu *et al.* [13] investigated the most optimal power allocation for Quality of Service (QoS) when it comes to ensuring weighted sum-rate maximization. For the pairing strategy of NOMA systems, the authors in [14] designed a scheme about user pairing according to the analytic expression for the pairing distance threshold with fixing power allocation. To mitigate the impact of SIC errors on legitimate users, Xiang *et al.* [15] proposed a power allocation scheme and analyzed the security and reliability of NOMA and OMA systems. In the wake of these papers, a number of dedicated cooperative NOMA schemes, denoted as relay-assisted cooperative NOMA networks, have been proposed in the quest to extend the coverage of the network and to obtain more diversity gains. For example, the authors of [16] considered a two-hop NOMA-based cooperative relay network and applied decode-and-forward and amplify-and-forward protocols to the selected relays. In order to assist in relaying device-to-device communication, Cai *et al.* proposed an optimal

power allocation strategy that aims to maximize ergodic sum-rate in [17]. In addition, intelligent reflective surface (IRS) was introduced due to the low cost, which can effectively adjust the direction of user channel vectors and facilitate the implementation of NOMA [18–20]. The authors of [18] improved the coverage of NOMA systems by deploying IRS to assist cell-edge user devices to communicate with base stations. With the aim of further enhancing network coverage, Zuo *et al.* [19] studied the resource allocation problem for IRS-NOMA systems transmitting in downlink. In [20], Zeng *et al.* considered the problem of sum rate maximization for uplink NOMA network with the assistance of IRS.

Security remains a key challenge for NOMA systems since the broadcast nature of wireless transmissions allows them prone to being accessed without authorization. There is a situation to be considered, where the content of the transmitted information cannot be protected, while only the transmission itself can be hidden [21]. In this case, traditional security schemes employing cryptography [22] and physical layer security (PLS) [23] are considered far from adequate, as such schemes can raise suspicions of adversaries, which can lead to further probing. To enhance the existing security approaches, a new proposition called covert communication has been recently proposed [24–27], which can hide the presence of wireless transmissions. In fact, as well as protecting the content of information in the present-day society and political environment, there is an urgent need to ensure the covertness of message delivery, for example, covert military operations, authoritarian government surveillance, intra-IoT interaction [28], etc. In addition, sensitive information about personal health issues or financial transactions falling into the hands of the wrong people could be used, which is extremely undesirable. In both above and a host of other communication environments, covert communication provides a feasible avenue of enhancing user privacy by being combined with current security methods [29].

Until recent years, the fundamental limits of covert communication have been described through an information-theoretic perspective. Bash *et al.* [24] presented the information-theoretic limits of covert communication over additive white Gaussian noise (AWGN) channels, namely the well-known Square Root Law (SRL). This ground-breaking work established the basis for research in information-theoretic on covert communication, pioneering two research directions that explored the fundamental limitations and feasibility of covert communication, respectively. Along the first direction, some researchers also extended SRL to a variety of other channel models, for instance, AWGN channels [30], binary symmetric channels [31], and discrete memoryless channels [32], etc. For example, Yan *et al.* [33] investigated covert communication with limited block length over AWGN channels and demonstrated that the effective covert throughput was optimal when all available channels were utilized. As a matter of fact, it can be easily seen from SRL that the average covert transmission bits used per channel in a covert system is asymptotically zero, but this does not mean that the covert communication system cannot achieve a positive transmission rate. Therefore, the second direction is developed, which allows to further develop the covertness performance for covert communication

by conducting feasibility studies. In slow fading channels, the authors in [34] analyzed covert communication with the assistance of multi-friendly cooperative nodes and proposed an opportunistic jammer selection scheme. To consider the effect of multiple interferences on covert communication, Yuda *et al.* [35] developed a public communication link using multi-antenna technologies to mask covert communication, while Shahzad *et al.* [36] considered covert communication in the existence of multi-antenna adversaries and delay constraints. Furthermore, covert communications with relay networks have been considered in [37] and [38], however, the authors of [39] enhanced the covert throughput in wireless networks by exploiting Poisson field interference.

A. Motivation and Contributions

Only a few studies on covert communication have been done in NOMA, and the related researches are able to be noted in [40–44]. In [40], the authors studied the covert communication performance in NOMA networks with AF relaying, where the relay was designed to detect covert transmissions and the transmitter hid covert transmissions by mixing covert messages with open messages from other users. To investigate the effect of a multi-antenna jammer with random power on covert NOMA communication, Peng *et al.* in [41] calculated the closed-form solution of average minimum detection error probability, and proposed an optimization scheme for maximizing the covert throughput. In the uplink NOMA system, the authors of [42] studied covert communication with the assistance of energy harvesting jammer, and analyzed the maximum effective covert rate (ECR) satisfying the QoS constraints. It is shown that there exists an optimal transmit power and time switch factor at Bob for maximizing the maximum ECR. While Wang *et al.* [43] utilized truncated channel inversion power control to achieve covert communication and proposed the optimal choice of power control parameters in order to achieve the maximum effective covert throughput. In the downlink NOMA system, the authors in [44] proposed a novel IRS-NOMA scheme that utilized the phase shift uncertainty of IRS and the non-orthogonal transmission of public users to act as a new coverage medium, and maximized Bob's covert rates with combined optimization of the transmitting power and IRS reflect beamforming.

Although previous contributions provide a solid basis for understanding NOMA techniques and covert communication, it still needs further research and development. To the authors' knowledge, the joint study of NOMA, covert communication and channel estimation errors have not been found in the open literature. The relevant studies can be found in reference [45] and [46]. The authors in [45] studied covert communication of block fading channels under condition of channel estimation errors, but did not focus on the combination of covert communication and NOMA. The authors in [46] considered covert communication in downlink NOMA systems, unfortunately, channel estimation errors were not considered. To this end, we study covert communication of downlink NOMA system by considering channel uncertainty. To improve system performance, a sub-optimal antenna selection technique scheme

is adopted at the transmitter for the strong NOMA users. In addition, we propose an optimization scheme that maximizes the covert throughput for the purpose of improving the system performance. The summary of the key contributions can be presented as below:

- In contrast to existing work, we consider channel estimation errors when implementing covert communication for downlink NOMA system and propose a k-th best transmitter antenna selection scheme. This occurs in the case that the optimal transmitting antenna is not available or has been scheduled.
- We derive the minimum detection error probability and its corresponding optimal detection threshold for warden in detecting covert communication behavior, and obtain a closed-form analytical solution for the expected minimum detection error probability (EMDEP). On this basis, an analysis of covertness performance is carried out.
- We also calculate the outage probability for two users and further bring the concept of covert throughput. For the sake of maximizing covertness performance of the considered system, we transform the covert throughput into an optimization problem. This optimization enables to obtain a maximum covert throughput with guaranteed covert constraints and interruption constraints, thus improving the covertness performance of the considered system.

B. Organization and Notations

The explicit arrangement of each of the remaining sections of this paper is displayed below. Section II introduces the NOMA-based covert communication system model considering channel uncertainty. Section III derives and explores the optimal detection threshold as well as minimum detection error probability for warden. Section IV investigates the covert throughput for the considered system and optimizes it. Section V verifies the correctness of the theoretical analysis by a number of simulation graphs. In the end, the conclusions of this article are provided in Section VI.

Notations: The $\mathcal{CN}\left(\mu, \sigma^2\right)$ indicates the complex Gaussian random variable with expectation μ and standard variance σ^2. $\mathbb{E}\left(\cdot\right)$ gets used to denote the expectation operation. $\Pr\left(\cdot\right)$ stands for the probability of a random variable. $\exp\left(\cdot\right)$ is used to represent the exponential function. The sign $|\cdot|$ means the absolute value of a scalar. In addition, $f_x\left(\cdot\right)$ is the mathematical expressions for probability density function (PDF). Finally, the permutation and combination of x and y are expressed as $\begin{pmatrix} x \\ y \end{pmatrix}$.

II. SYSTEM MODEL

A. Communication Scenario

Considering a downlink NOMA system as shown in Fig. 1, in which the transmitter (Alice) sends public messages to the weak user (Carl). Alice also intends to send a message towards the strong user (Bob) with the aim of hiding this
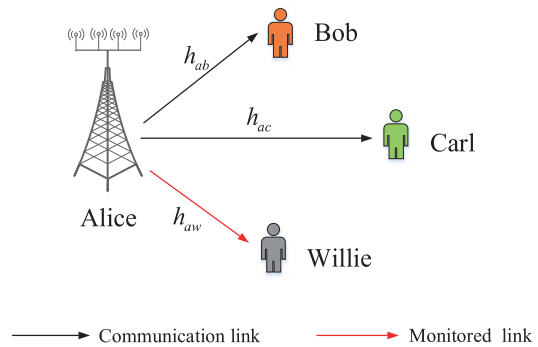

Fig. 1.   System model.

communication from the warden (Willie). It is noted that low-power signals are suitable for covert information, while high-power signals are suitable as interference. Therefore, the covert transmission between Alice and Bob is considered while using the transmission to Carl as its cover in this study. A passive detection of whether Alice is also sending messages to Bob is performed by Willie. Assuming that the transmitting power used by Alice is known to Willie, and Willie plays with a radiometer (power detector) as its detector. For convenience, it is also assumed that Alice is configured with N_t antennas and the rest of the nodes are single-antenna devices operating in half-duplex (HD) mode.

In the considered system, each of the wireless channels is assumed to obey independent quasi-static Rayleigh fading channels, and the channel coefficients are independent and identically distributed (i.i.d.) circularly symmetric complex Gaussian random variables. The channel fading coefficients between the i-th $(1 \leq i \leq N_t)$ antenna of Alice and Bob, Carl, and Willie all obey zero mean and unit variance, i.e., $h_{ab}^i \sim \mathcal{CN}\left(0, 1\right)$, $h_{ac}^i \sim \mathcal{CN}\left(0, 1\right)$, and $h_{aw}^i \sim \mathcal{CN}\left(0, 1\right)$. The distances from Alice to Bob, Alice to Carol, and Alice to Willie can be represented as d_{ab}, d_{ac} and d_{aw}, respectively. It is assumed that the channel state information (CSI) of Bob and Carl are known, while Alice only knows the statistical CSI of Willie.

B. Antenna Transmission Solution

Alice first performs antenna selection before sending a message. In this system, Alice adopts a sub-optimal antenna selection algorithm to select the k-th best antenna to send a message to Bob. The sub-optimal antenna selection algorithm does not select the best antenna all at once, but the k-th best antenna in the order of performance from best to worst among the antennas, and the k-th best antenna selected is denoted as

$$k = k_{th} \underset{1 \leq i \leq N_t}{\arg\max} \left(\gamma_{ab}^i\right), \tag{1}$$

where $1 \leq k \leq N_t$, γ_{ab}^i denotes the signal-to-noise ratio (SNR) from the i-th antenna of Alice to Bob. When $k = 1$, the optimal antenna is selected. When $k = N_t$, the worst antenna is selected. The channel coefficient between the k-th best antenna of Alice and Bob is expressed as h_{ab}^k. The PDF of $\left|h_{ab}^k\right|^2$ can be written as [47]

$$f_{\left|h_{ab}^k\right|^2}(x) = (N_t - k + 1) \begin{pmatrix} N_t \\ N_t - k + 1 \end{pmatrix} \\ \times \left(1 - e^{-x}\right)^{N_t - k} \left(e^{-x}\right)^k. \qquad (2)$$

C. Transmission Phase

While constantly sending legitimate messages to Carl, Alice may send a covert message to Bob at a specific block of time. There is a pre-shared secret between Alice and Bob, which enables Bob to learn in advance the block which Alice has chosen and thus receive the message exactly.

When Alice sends a covert message to Bob, it transmits a superimposed message $x = \sqrt{(1 - \varphi) P_a} x_1 + \sqrt{\varphi P_a} x_2$ to a predefined NOMA user pair (Bob, Carl), based on statistical CSI, where P_a is used to denote the total transmitting power transmitted by Alice, φ denotes Alice's power allocation factor. In general, weak users are given more power than strong users for the purpose of ensuring system performance and fairness between users. Since Bob is a strong user, $0 < \varphi \leq 0.5$. x_1 and x_2 are the signals corresponding to Carl and Bob, where $\mathbb{E}\left(|x_1|^2\right) = \mathbb{E}\left(|x_2|^2\right) = 1$. Therefore, the received signal at Bob can be obtained as

$$y_b(n) = h_{ab}^k \left(\sqrt{(1 - \varphi) P_a} x_1(n) \\ + \sqrt{\varphi P_a} x_2(n)\right) d_{ab}^{-\alpha/2} + n_b(n) \quad, \qquad (3)$$

where $n = 1, 2, \ldots, N$, where N is the total number of channels used. α is expressed as the path loss exponent. $n_b(n) \sim \mathcal{CN}\left(0, \sigma_b^2\right)$ represents the AWGN at Bob.

In practice, the perfect CSI is not be available due to channel estimation errors. To obtain CSI, the linear minimum mean square error is applied, so the channel coefficient is modelled as [48, 49]

$$h_s = \hat{h}_s + e_s, \qquad (4)$$

where $s \in (aw, ac, ab)$, $e_s \sim \mathcal{CN}(0, \beta_s)$ and $\hat{h}_s \sim \mathcal{CN}(0, 1 - \beta_s)$ denote the channel estimation errors and estimated channel of the real channel h_s, respectively, which are zero-mean, independent circularly symmetric complex Gaussian random variables. Therefore, Eq. (3) is given by

$$y_b(n) = \left(\hat{h}_{ab}^k + e_{ab}^k\right) \left(\sqrt{(1 - \varphi) P_a} x_1(n) \\ + \sqrt{\varphi P_a} x_2(n)\right) d_{ab}^{-\alpha/2} + n_b(n) \quad, \qquad (5)$$

where $\hat{h}_{ab}^k$ and e_{ab}^k are the known and uncertain parts of Bob's channel from Alice.

III. OPTIMAL DETECTION AT WILLIE

In this section, we explore the signal received by Willie. To gain more insight, its detection error probability and optimal detection threshold are calculated and analyzed.

A. Detection Performance at Willie

For a time slice of communication, a binary hypothesis testing problem with respect to whether Alice sends a covert signal to Bob is presented to Willie, with the null hypothesis H_0 indicating that only public messages are being transmitted and the alternative hypothesis H_1 indicating that a covert message is sent by Alice to Bob. Under both of the two hypotheses, the received signal at Willie is represented, respectively, as

$$H_0: \quad y_w(n) = \left(\hat{h}_{aw}^k + e_{aw}^k\right) \sqrt{(1 - \varphi) P_a} x_1(n) \\ \times d_{aw}^{-\alpha/2} + n_w(n) \quad, \qquad (6)$$

$$H_1: \quad y_w(n) = \left(\hat{h}_{aw}^k + e_{aw}^k\right) \left(\sqrt{(1 - \varphi) P_a} x_1(n) \\ + \sqrt{\varphi P_a} x_2(n)\right) d_{aw}^{-\alpha/2} + n_w(n) \quad, \qquad (7)$$

where $n_w(n)$ is determined as AWGN at Willie and follows a circularly symmetric complex Gaussian distribution with a mean of zero and variance of σ_w^2, that is $n_w(n) \sim \mathcal{CN}\left(0, \sigma_w^2\right)$.

Willie uses a radiometer for detection and analyzes the received signal. The judgments made by Willie that Alice is not sending a covert message and there is a communication behavior between Alice and Bob, which is determined as D_0 and D_1, respectively. Based on the Neyman-Pearson criterion, the Likelihood Ratio test is the optimal decision rule for minimization of the total detection error probability of Willie [50], which can be translated into a test of the average received power at the receiver over a time period. Thus for a radiometer, the optimal decision rule can be given by [51]

$$Y_w \underset{D_0}{\overset{D_1}{\gtrless}} \tau, \qquad (8)$$

where the test statistic $Y_w = \frac{1}{N} \sum_{n=1}^N |y_w(n)|^2$ is Willie's average received power over a time slot and $\tau > 0$ is the predefined detection threshold of the detector. In this study, we consider the use of an infinite number of channels, i.e., $N \to \infty$. Therefore, Y_W is given by

$$Y_w = \begin{cases} \left|\hat{h}_{aw}^k\right|^2 (1 - \varphi) P_a d_{aw}^{-\alpha} \\ + \left|e_{aw}^k\right|^2 (1 - \varphi) P_a d_{aw}^{-\alpha} + \sigma_w^2, & H_0, \\ \left|\hat{h}_{aw}^k\right|^2 P_a d_{aw}^{-\alpha} + \left|e_{aw}^k\right|^2 P_a d_{aw}^{-\alpha} + \sigma_w^2, & H_1. \end{cases} \qquad (9)$$

Willie must make a decision about Alice's communication behavior when a certain time slot comes to an end. We define the *false alarm* probability (FAP) as the probability that the real occurrence is H_0 whereas Willie makes a decision favoring H_1, denoted as $\mathbb{P}_{fa} = \Pr(D_1 | H_0)$. In a similar way, the *miss detection* probability (MDP) can be described as the probability that Alice and Bob do communicate covertly and Willie decides that there is no communication between the parties, which is denoted as $\mathbb{P}_{md} = \Pr(D_0 | H_1)$. With the hypothesis that H_0 and H_1 have equal prior probabilities, it is necessary to analyze detection performance of Willie for

assessing the level of covert communication. The detection error probability at Willie is denoted as

$$\xi = \mathbb{P}_{fa} + \mathbb{P}_{md}, \qquad (10)$$

when ε is small enough, $\varepsilon > 0$, all $\xi \geq 1 - \varepsilon$ are valid, it can be considered that Alice successfully sends a covert signal to Bob and the signal has not been detected by Willie.

B. False Alarm and Miss Detection Probability

Lemma 1. *Willie's FAP and MDP can be written as*

$$\mathbb{P}_{fa} = \begin{cases} e^{-\frac{\tau - \psi_1}{\beta_{aw} A_1}}, & \tau \geq \psi_1, \\ 1, & \tau < \psi_1, \end{cases} \qquad (11)$$

and

$$\mathbb{P}_{md} = \begin{cases} 1 - e^{-\frac{\tau - \psi_2}{\beta_{aw} A_2}}, & \tau \geq \psi_2, \\ 0, & \tau < \psi_2, \end{cases} \qquad (12)$$

respectively, where $\psi_1 = A_1 \left| \hat{h}_{aw}^k \right|^2 + \sigma_w^2$, $\psi_2 = A_2 \left| \hat{h}_{aw}^k \right|^2 + \sigma_w^2$, $A_1 = (1 - \varphi) P_a d_{aw}^{-\alpha}$, $A_2 = P_a d_{aw}^{-\alpha}$.

Proof: See Appendix A. ∎

Lemma 2. *Willie's detection error probability can be written as*

$$\xi = \begin{cases} 1, & \tau < \psi_1, \\ e^{-\frac{\tau - \psi_1}{\beta_{aw} A_1}}, & \psi_1 \leq \tau \leq \psi_2, \\ 1 - e^{-\frac{\tau - \psi_2}{\beta_{aw} A_2}} + e^{-\frac{\tau - \psi_1}{\beta_{aw} A_1}}, & \tau > \psi_2. \end{cases} \qquad (13)$$

Proof: Eq. (13) can be obtained by bringing Eqs. (11) and (12) into Eq. (10). ∎

C. Optimal Detection Threshold

In this section, we derive the optimal value of the detection threshold for minimizing detection error probability at Willie and minimum detection error probability.

Theorem 1. *With the above metrics for Willie in mind, the optimal detection threshold is expressed as*

$$\tau^* = \begin{cases} \Delta_1, & \text{if} \left| \hat{h}_{aw}^k \right|^2 < \Delta_2, \\ \psi_2, & \text{otherwise,} \end{cases} \qquad (14)$$

where $\Delta_1 = \frac{A_1 A_2 \beta_{aw}}{A_1 - A_2} \ln \left(\frac{A_1}{A_2} e^{\frac{(A_1 - A_2)\sigma_w^2}{A_1 A_2 \beta_{aw}}} \right)$, $\Delta_2 = \frac{\Delta_1 - \sigma_w^2}{A_2}$.

The minimum detection error probability can be derived as

$$\xi^* = \begin{cases} 1 - e^{-\frac{\Delta_1 - \psi_2}{\beta_{aw} A_2}} + e^{-\frac{\Delta_1 - \psi_1}{\beta_{aw} A_1}}, & \text{if} \left| \hat{h}_{aw}^k \right|^2 < \Delta_2, \\ e^{-\frac{\psi_2 - \psi_1}{\beta_{aw} A_1}}, & \text{otherwise.} \end{cases} \qquad (15)$$

Proof: From the standpoint of Willie, it is necessary to identify the optimal detection threshold for minimizing its detection error probability, which is defined as

$$\tau^* = \arg \min_{\tau} \xi. \qquad (16)$$

According to Eq. (13), it is clear that Willie will not set τ at $(0, \psi_1)$. Next, there are two remaining cases that we analyze and study the optimal value of τ allowing ξ to be minimized.
Case 1: $\psi_1 \leq \tau \leq \psi_2$

From Eq. (13), One can see that ξ decreases as τ grows larger. Therefore, Willie can choose the highest possible value of τ as the optimal threshold, i.e., $\tau^* = \psi_2$. By substituting τ^* into Eq. (13), we get $\xi^* = e^{-\frac{\psi_2 - \psi_1}{\beta_{aw} A_1}}$.
Case 2: $\tau > \psi_2$

As a way to determine the optimal value of τ in this case, we find the first order derivative of ξ with respect to τ and make it equal to 0, which is expressed as

$$\frac{\partial \xi}{\partial \tau} = \frac{1}{\beta_{aw} A_2} e^{-\frac{\tau - \psi_2}{\beta_{aw} A_2}} - \frac{1}{\beta_{aw} A_1} e^{-\frac{\tau - \psi_1}{\beta_{aw} A_1}} = 0. \qquad (17)$$

After some simple manipulations of Eq. (17), the optimum value of τ is represented as

$$\Delta_1 = \frac{A_1 A_2 \beta_{aw}}{A_1 - A_2} \ln \left(\frac{A_1}{A_2} e^{\frac{(A_1 - A_2)\sigma_w^2}{A_1 A_2 \beta_{aw}}} \right). \qquad (18)$$

We note that Δ_1 is expressed as the extreme value point of ξ. It can be confirmed by the second order derivative of ξ with respect to τ, which is written as

$$\frac{\partial^2 \xi}{\partial \tau^2} = -\frac{1}{\beta_{aw}^2 A_2^2} e^{-\frac{\tau - \psi_2}{\beta_{aw} A_2}} + \frac{1}{\beta_{aw}^2 A_1^2} e^{-\frac{\tau - \psi_1}{\beta_{aw} A_1}}, \qquad (19)$$

If we replace Δ_1 in Eq. (19) to obtain $\frac{\partial^2 \xi}{\partial \tau^2} > 0$, we can prove that Δ_1 is a minimal value point of ξ and there is a minimal value ξ^* of ξ, which is expressed as

$$\xi^* = 1 - e^{-\frac{\Delta_1 - \psi_2}{\beta_{aw} A_2}} + e^{-\frac{\Delta_1 - \psi_1}{\beta_{aw} A_1}}. \qquad (20)$$

Thus, Δ_1 denotes the optimal threshold for ξ provided when $\Delta_1 > \psi_2$ is satisfied. If Δ_1 does not satisfy this condition, for $\tau > \Delta_1$, ξ is a monotonically increasing function with an optimal threshold of $\tau^* = \psi_2$, the same as in *Case 1*.

As a conclusion, the optimal detection threshold and the minimum detection error probability for Willie can be shown in Eqs. (14) and (15). ∎

Remark 1. *First of all, it is obvious from Eq. (15) that ξ^* has nothing to do with σ_w^2, because Willie learns it on the basis of multiple observations. If there is no channel estimation errors, Willie can also track the transmit power by observing. To solve this problem, it is assumed that all channels in the system have estimation errors. Secondly, when the channel gain $\left| \hat{h}_{aw}^k \right|^2$ is much smaller than Δ_2, that is, when Δ_1 is much larger than ψ_2, $\xi^* = 1 - e^{-\frac{\Delta_1}{\beta_{aw} A_2}} + e^{-\frac{\Delta_1}{\beta_{aw} A_1}}$, ξ^* and Δ_1 are positively correlated. When $\left| \hat{h}_{aw}^k \right|^2 \geq \Delta_2$, ξ^* has nothing to do with Δ_1. Interestingly, we observe mathematically that Δ_1 is independent of $\hat{h}_{aw}^k$, which can be explained by understanding*

the occurrence of Δ_1, i.e., Δ_1 is a function consisting of large-scale fading and transmitting power, and therefore it is not related to small-scale fading $\hat{h}_{aw}^k$.

IV. PERFORMANCE OF COVERT COMMUNICATIONS

In this section, we start with an analysis of the outage probabilities at Bob and Carl. Secondly, we optimize the maximum covert throughput of the system under certain covertness constraints and reliability constraints.

A. Outage probability

With the SIC in NOMA, the signal from Carl is firstly decoded by Bob, then eliminated from the received signal, and lastly Bob's own signal is detected. Thus, the received signal-to-interference-plus-noise ratio (SINR) of the signal x_1 of Carl detected at Bob can be represented as

$$\gamma_{c \to b} = \frac{(1-\varphi)P_a \left| \hat{h}_{ab}^k \right|^2}{\varphi P_a \left| \hat{h}_{ab}^k \right|^2 + P_a \left| e_{ab}^k \right|^2 + d_{ab}^\alpha \sigma_b^2}. \tag{21}$$

In the case of $\gamma_{c \to b} > 2^{R_1} - 1$, Bob can correctly detect x_1. We note that when Bob cannot successfully decode x_1, Bob cannot be able to decode x_2 correctly. This is because the SINR of x_2 is lower than the SINR of x_1 at Bob, while the transmission rate of x_2 is not less than that of x_1. The SINR of x_2 following the SIC is given by

$$\gamma_b = \frac{\varphi P_a \left| \hat{h}_{ab}^k \right|^2}{P_a \left| e_{ab}^k \right|^2 + d_{ab}^\alpha \sigma_b^2}. \tag{22}$$

The SINR of x_1 detected at Carl can be obtained as

$$\gamma_c = \frac{(1-\varphi)P_a \left| \hat{h}_{ac}^k \right|^2}{\varphi P_a \left| \hat{h}_{ac}^k \right|^2 + P_a \left| e_{ac}^k \right|^2 + d_{ac}^\alpha \sigma_c^2}, \tag{23}$$

where σ_c^2 is the variance of AWGN at Carl.

Next, we derive the outage probabilities to evaluate the reliability of the considered system.

Theorem 2. *The outage probabilities for Bob and Carl are respectively denoted as*

$$\delta_b = g^2 \binom{N_t}{g}^2 \sum_{i=0}^{g-1} \sum_{j=0}^{g-1} \binom{g-1}{i} \binom{g-1}{j} (-1)^{i+j}$$
$$\times \frac{1}{\lambda_1} \left[\frac{1}{\lambda_2} - \frac{1-\beta_{ab}}{\lambda_2 - \lambda_2 \beta_{ab} + \lambda_1 \Phi_2 P_a \beta_{ab}} e^{\frac{\lambda_1 D_1 \Phi_2}{1-\beta_{ab}}} \right], \tag{24}$$

and

$$\delta_c = 1 - \frac{1-\beta_{ac}}{\Phi_1 P_a \beta_{ac} + 1 - \beta_{ac}} e^{-\frac{\Phi_1 D_2}{1-\beta_{ac}}}, \tag{25}$$

where $g = N_t - k + 1$, $\mu_1 = 2^{R_1} - 1$, $\mu_2 = 2^{R_2} - 1$ *(i.e., R_1 and R_2 are predetermined rates for Alice to Carl and Bob, respectively.).* $\Phi_1 = \frac{\mu_1}{(1-\varphi-\mu_1\varphi)P_a}$, $\Phi_2 = \frac{\mu_2}{\varphi P_a}$, $\lambda_1 = -k - i$, $\lambda_2 = -k - j$, $D_1 = d_{ab}^\alpha \sigma_b^2$, $D_2 = d_{ac}^\alpha \sigma_c^2$.

Proof: See Appendix B. ■

Corollary 1. *In the high SNR case, the asymptotic expressions for the outage probability of Bob and Carl can be expressed as*

$$\delta_b^\infty = g^2 \binom{N_t}{g}^2 \sum_{i=0}^{g-1} \sum_{j=0}^{g-1} \binom{g-1}{i} \binom{g-1}{j} (-1)^{i+j}$$
$$\times \frac{1}{\lambda_1} \left[\frac{1}{\lambda_2} - \frac{1-\beta_{ab}}{\lambda_2 - \lambda_2 \beta_{ab} + \lambda_1 \Phi_2 P_a \beta_{ab}} \right], \tag{26}$$

and

$$\delta_c^\infty = 1 - \frac{1-\beta_{ac}}{\Phi_1 P_a \beta_{ac} + 1 - \beta_{ac}}, \tag{27}$$

respectively. δ_b^∞ and δ_c^∞ are constants.

Proof: Considering Bob's outage probability in the high SNR region, it is clear that $P_a \to \infty$, i.e., $\Phi_2 \to 0$, so $e^{\frac{\lambda_1 D_1 \Phi_2}{1-\beta_{ab}}} \to 1$, thus the asymptotic expression for the outage probability of Bob is shown in Eq. (26). Similarly, $\Phi_1 \to 0$, $e^{-\frac{D_2 \Phi_1}{1-\beta_{ac}}} \to 1$, so Carl's asymptotic expression for outage probability is displayed in Eq. (27). ■

B. Expected minimum detection error probability

Given that the instantaneous CSI associated with Willie is not known to Alice and Bob, they are obliged to obtain feasible covertness by relying on the expectation of the minimum detection error probability.

Theorem 3. *The EMDEP with the optimal detection threshold is given by*

$$\bar{\xi}^* = \left[1 - \frac{\beta_{aw}}{1-2\beta_{aw}} \left(\kappa_2 - \kappa_2^{\frac{1}{\kappa_1}} - e^{-\frac{\Delta_2}{\beta_{aw}}} + e^{\frac{\sigma_w^2 - \Delta_1}{A_1 \beta_{aw}}} \right) \right] \times \kappa_1 \kappa_2^{\frac{\kappa_1+1}{\kappa_1}} (1 - \kappa_2), \tag{28}$$

where $\kappa_1 = \frac{A_1 \beta_{aw}}{A_2(1-\beta_{aw}) + A_1(2\beta_{aw} - 1)}$, $\kappa_2 = e^{\frac{\Delta_2}{(\beta_{aw}-1)}}$.

Proof: See Appendix C. ■

C. Covert Throughput

1) Covert throughput: Based on the channel throughput for covert message transmission from Alice to Bob, the covert throughput is determined as $\Gamma = (1 - \delta_b)R_2$.

2) Covert throughput maximization: The objective of covert throughput maximization deals with maximizing the covert throughput while maintaining a sufficiently high-probability of detection errors at Willie. We can state covert throughput maximization as an optimization problem, which can be denoted by

$$\max_{\varphi P_a} \Gamma = (1 - \delta_b) R_2,$$
$$s.t. \quad \bar{\xi}^* \geq 1 - \varepsilon, \tag{29}$$
$$\delta_c \leq \delta_{th},$$

Fig. 2. $\mathbb{P}_{fa}$, $\mathbb{P}_{md}$ and ξ at different values of τ.

Fig. 3. EMDEP $\bar{\xi}^*$ vs. β_{aw} for different values of P_a and φ.
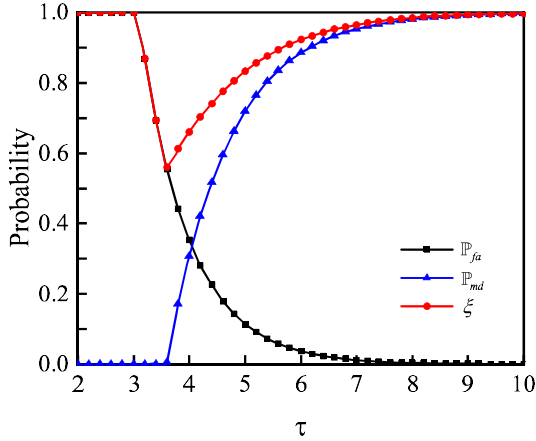
where $\bar{\xi}^* \geq 1 - \varepsilon$ represents the covertness constraint of the considered system. δ_{th} denotes the predetermined maximum outage probability value.

Remark 2. *There are three steps to address the optimization problem: 1) When satisfying the covertness constraint in Eq. (29), it is capable of finding a maximum value φ^* since Alice's transmitting power P_a has no effect on EMDEP; 2) The reliability constraint by substituting φ^* into Eq. (29) yields a minimum of P_a, i.e., $P_a^{\min}$. This indicates that the transmission of information between Alice and Carl is ensured as long as Alice uses a transmitting power greater than $P_a^{\min}$; 3) The maximum covert throughput of Bob is obtained by bringing φ^* and any P_a $\left(P_a \geq P_a^{\min} \right)$ into the expression for the covert throughput. It is to be noted that the maximum covert through-put of Bob converges to a constant when P_a $\left(P_a \geq P_a^{\min} \right)$ reaches a certain value.*

Corollary 2. *In the high SNR case, the asymptotic expression for the covert throughput is given by*

$$\Gamma^\infty = \left(1 - \delta_b^\infty \right) R_2. \tag{30}$$

Γ^∞ *remains fixed, so that the asymptotic value of the maximum covert throughput satisfying Eq. (29) is also a fixed constant Γ_m^∞.*

V. RESULTS AND DISCUSSIONS

In this section, numerical results are used to prove the correctness of the system performance analysis in Sections III and IV. In all simulations, except where explicitly stated otherwise, it was assumed that the system parameter settings for these results as follow: $d_{ab} = d_{aw} = 3$, $d_{ac} = 4$, $\alpha = 3$, $\sigma_b^2 = \sigma_c^2 = \sigma_w^2 = 1$, $R_1 = 0.1$, $R_2 = 0.2$.

Fig. 2 shows the variation curves of FAP $\mathbb{P}_{fa}$, MDP $\mathbb{P}_{md}$ and detection error probability ξ for different detection thresholds τ. We set $\varphi = 0.2$, $\beta_{aw} = 0.30$, $P_a = 20$ dB. We can observe that the FAP $\mathbb{P}_{fa}$ at Willie first stays at 1, and as τ increases, $\mathbb{P}_{fa}$ decreases linearly and eventually stays at 0. In contrast, the MDP $\mathbb{P}_{md}$ at Willie tends to be infinitely close
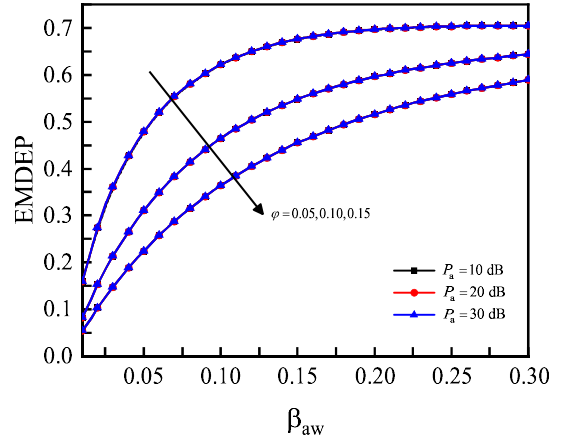
to 1 as τ increases. Moreover, we learn that detection error probability ξ is the sum of $\mathbb{P}_{fa}$ and $\mathbb{P}_{md}$. Since τ is relatively small, the former dominates ξ, causing ξ to decrease with τ. However, it is the latter that dominates ξ when τ increases further, which leads to an increase in ξ. As illustrated in Fig. 2, there exists a minimum ξ, whose corresponding τ is the optimal detection threshold. With this minimum ξ, Willie is most capable of discovering the transmission between Alice and Bob.

Fig. 3 depicts the EMDEP $\bar{\xi}^*$ versus the channel estimation errors β_{aw} for different transmitting power P_a and power allocation factors φ. As can be seen from Fig. 3, $\bar{\xi}^*$ increases gradually as β_{aw} increases and then converges to a constant value. This shows that appropriate channel estimation errors are very effective in interfering with the detection at Willie. Furthermore, it is observed that the power allocation factor φ also has an effect on Willie's EMDEP, i.e., $\bar{\xi}^*$ decreases with the increase of φ. This is because the larger the φ, the greater the transmitting power allocated to Bob by Alice and thus the greater the probability of covert communication behavior being detected by Willie. It is worth noting that when φ and β_{aw} are held constant, P_a has no effect on EMDEP.

In Fig. 4, we show the relationship between outage probability and the transmitting power P_a of Alice for different channel estimation errors $\beta = \{\beta_{ab}, \beta_{ac}\}$. We set $\varphi = 0.2$, $N_t = 5$, and $k = 1$. We begin by analyzing the outage probability for Bob. From this figure, it can be seen that outage probability decreases monotonically with P_a, i.e., the higher the transmitting power of Alice, the smaller the outage probability of the system. As P_a increases, the outage probability decreases slowly and converges to a lower limit. As shown in **Corollary 1**, the asymptotic value of outage probability is a constant. We can also find in the figure that outage probability increases with β when P_a is constant, which indicates that the channel estimation errors reduces the reliability performance of the system. The analysis of outage probability by Carl is similar to that of Bob.

In Fig. 5, outage probability is plotted versus P_a when Alice picks different number of antennas, $k = \{1, 3, 5\}$. We set
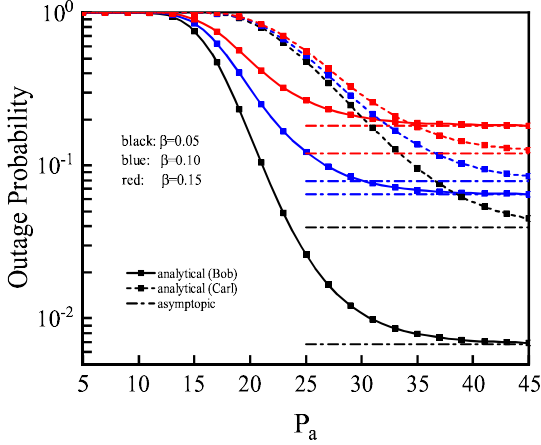
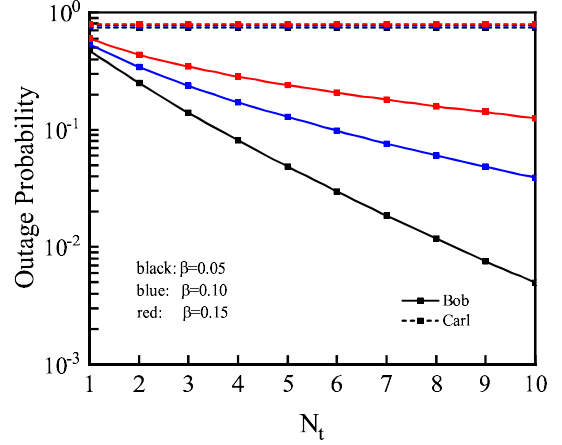Fig. 4. outage probability vs. P_a for different values of β.

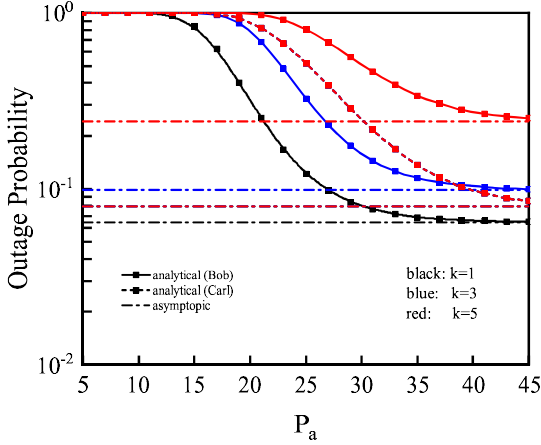Fig. 6. outage probability for different values of β vs. N_t.

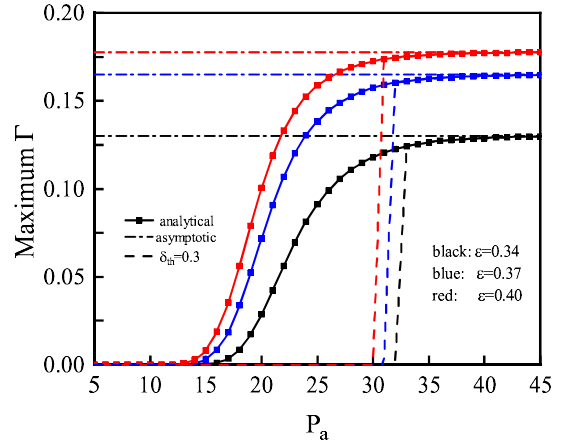Fig. 5. outage probability for different values of k vs. P_a.

Fig. 7. Maximum covert throughput Γ vs. P_a with different values of ε.

$\varphi = 0.2$, $\beta = 0.10$, and $N_t = 5$. When P_a is constant, the smaller k is, the better outage probability performance from the standpoint of Bob. This is due to the fact that a smaller k indicates a better antenna selected by Alice, making the Alice-to-Bob communication of higher quality and less prone to outage events. However, the outage probability for Carl is not relevant to k.

Fig. 6 illustrates the relationship between outage probability and the number of transmitting antennas N_t for different channel estimation errors $\beta = \{\beta_{ab}, \beta_{ac}\}$. Some parameters are set as follows: $P_a = 20$ dB, $\varphi = 0.3$, $k = 1$. It should be noted that Alice selects the optimal transmitting antenna when $k = 1$. After observing the simulation figure, we can see that the outage probability of Bob becomes significantly better with the increase of N_t after Alice performs the optimal antenna selection scheme. However, as N_t increases, the performance improvement decreases gradually, therefore, N_t needs to be selected reasonably based on the system power consumption and performance requirements. Whereas, Carl's outage probability is independent of N_t. Furthermore, one can observe that the outage probability of both Bob and Carl

increases with the increase of β, which remains consistent with the analysis in Fig. 4.

Fig. 7 demonstrates the variation curve of the maximum covert throughput Γ versus Alice's transmitting power P_a for different covertness constraints ε. We set: $\beta_{aw} = 0.30$, $\beta_{ab} = \beta_{ac} = 0.10$, $N_t = 10$, $k = 1$. Without considering Carl's reliability constraint, we first notice that Γ increases monotonically with P_a, which indicates that covert communication between Alice and Bob becomes easier as the transmitting power of Alice increases. When $P_a \to \infty$, we also take note that the maximum Γ converges to a fixed constant Γ_m^∞ as shown in **Corollary 2**, which is attributed to the fact that the increase in the transmitting power of Alice not only enhances the quality of the communication between Alice and Bob, but also improves the probability of Willie detecting the covert communication. Besides, we also note that the top limit of maximum Γ increases as ε rises, since an increase in ε implies a smaller covert demand, which allows more covert messages to be transmitted. By taking the reliability constraint at Carl into account, we find that maximum covert throughput exists only when P_a is larger than a certain value, which is a
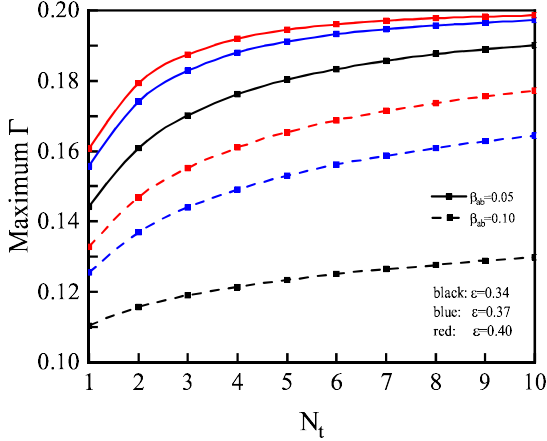
Fig. 8. Maximum covert throughput Γ_1 vs. N_t with different values of β_{ab} and ε.

result that also nicely validates **Remark 2**.

In Fig. 8, we show the maximum covert throughput Γ versus the number of transmitting antennas N_t for different channel estimation errors β_{ab} and covertness constraints ε. From Fig. 7, we can obtain the P_a corresponding to the maximum Γ tangent to its asymptote, at which point increasing P_a has almost no effect on maximizing Γ, so we set P_a in Fig. 8 to the same value. The simulation curves in Fig. 8 display that as N_t increases, the maximum Γ increases as well. However, the magnitude of performance improvement decreases as the number of transmitting antennas rises. Therefore, it is necessary to choose the number of transmitting antennas reasonably by integrating the power consumption and performance requirements of the considered system, and blindly increasing the number of transmitting antennas cannot continuously enhance the covertness performance of the system to a large extent. Moreover, it is further observed that the larger the β_{ab} is, the smaller the maximum Γ is, which is consistent with the analysis we conducted earlier.

VI. CONCLUSION

In this paper, we study the performance of covert communication in a downlink NOMA system considering users who are uncertain about their channel. To improve the transmission performance of the considered system, a suboptimal antenna selection scheme is used on Alice. We derive closed expressions for Willie's minimum detection error probability, the optimal detection threshold, and EMDEP, as well as the exact expressions for the outage probability of the two users. Based on this, we perform an optimization of the covert throughput. Numerical results demonstrate that it is possible to improve the maximum covert throughput of the considered system through an increased number of antennas and transmitting power. Furthermore, the selection scheme of the k-th best antenna can solve the problem of unavailability of the optimal antenna, as well as Willie's detection performance can be reduced by increasing the channel estimation errors. Finally,

we are able to conclude that the system is capable of achieving a degree of covert communication.

APPENDIX A

Combined with Eq. (9), the FAP can be expressed as

$$
\begin{aligned}
\mathbb{P}_{fa} &= \Pr\left(Y_w > \tau \,|\, H_0\right) \\
&= \Pr\left(A_1 \left|\hat{h}_{aw}^k\right|^2 + A_1 \left|e_{aw}^k\right|^2 + \sigma_w^2 > \tau\right) \\
&= \begin{cases} \Pr\left(\left|e_{aw}^k\right|^2 > \dfrac{\tau - \psi_1}{A_1}\right), & \tau \geq \psi_1, \\ 1, & \tau < \psi_1. \end{cases}
\end{aligned} \tag{A.1}
$$

In a similar way, the MDP is denoted by

$$
\begin{aligned}
\mathbb{P}_{md} &= \Pr\left(Y_w < \tau \,|\, H_1\right) \\
&= \Pr\left(A_2 \left|\hat{h}_{aw}^k\right|^2 + A_2 \left|e_{aw}^k\right|^2 + \sigma_w^2 < \tau\right) \\
&= \begin{cases} \Pr\left(\left|e_{aw}^k\right|^2 < \dfrac{\tau - \psi_2}{A_2}\right), & \tau \geq \psi_2, \\ 0, & \tau < \psi_2. \end{cases}
\end{aligned} \tag{A.2}
$$

After some algebraic operations, **Lemma 1** can be obtained.

APPENDIX B

The outage event will occur for Bob in two cases: 1) Bob cannot successfully decode x_1 (P_1); 2) Bob can successfully decode x_1, but cannot decode the desired signal (P_2). Therefore, the outage probability for Bob is $\delta_b = P_1 + P_2$. P_1 and P_2 are denoted as

$$
\begin{aligned}
P_1 &= \Pr\left(\gamma_{c \to b} < \mu_1\right) \\
&= \int_0^\infty \int_0^{\Phi_1(P_a y + D_1)} f_{\left|\hat{h}_{ab}^k\right|^2}(x) f_{\left|e_{ab}^k\right|^2}(y)\, dx dy
\end{aligned}, \tag{B.1}
$$

and

$$
\begin{aligned}
P_2 &= \Pr\left(\gamma_b < \mu_2, \gamma_{c \to b} \geq \mu_1\right) \\
&= \int_0^\infty \int_{\Phi_1(P_a y + D_1)}^{\Phi_2(P_a y + D_1)} f_{\left|\hat{h}_{ab}^k\right|^2}(x) f_{\left|e_{ab}^k\right|^2}(y)\, dx dy
\end{aligned}. \tag{B.2}
$$

Similarly, Carl's outage probability is given by

$$
\begin{aligned}
\delta_c &= \Pr\left(\gamma_c < \mu_1\right) \\
&= \int_0^\infty \int_0^{\Phi_1(P_a y + D_2)} f_{\left|\hat{h}_{ac}^k\right|^2}(x) f_{\left|e_{ac}^k\right|^2}(y)\, dx dy
\end{aligned}. \tag{B.3}
$$

The proof of **Theorem 2** can be obtained after some calculations.

$$\mathbb{E}\left(\xi^*\left|\left|\hat{h}_{aw}^k\right|\right|^2 < \Delta_2\right) = \int_0^{\Delta_2}\left(1 - e^{-\frac{\Delta_1 - \sigma_w^2 - \Lambda_2 x}{\Lambda_2 \beta_{aw}}} + e^{-\frac{\Delta_1 - \sigma_w^2 - \Lambda_1 x}{\Lambda_1 \beta_{aw}}}\right)f_{\left|\hat{h}_{aw}^k\right|^2}(x)\,dx$$
$$= 1 - \frac{1}{1 - \beta_{aw}}\int_0^{\Delta_2} e^{\frac{\left(\sigma_w^2 - \Delta_1\right)(1 - \beta_{aw}) + (1 - 2\beta_{aw})\Lambda_2 x}{\Lambda_2 \beta_{aw}(1 - \beta_{aw})}} - e^{\frac{\left(\sigma_w^2 - \Delta_1\right)(1 - \beta_{aw}) + (1 - 2\beta_{aw})\Lambda_1 x}{\Lambda_1 \beta_{aw}(1 - \beta_{aw})}}\,dx \tag{C.2}$$

APPENDIX C

Based on Eq. (15), the EMDEP is represented as

$$\begin{aligned}\bar{\xi}^* = &\ \mathbb{E}\left(\xi^*\left|\left|\hat{h}_{aw}^k\right|\right|^2 < \Delta_2\right)\Pr\left(\left|\hat{h}_{aw}^k\right|^2 < \Delta_2\right)\\ &+ \mathbb{E}\left(\xi^*\left|\left|\hat{h}_{aw}^k\right|\right|^2 \geq \Delta_2\right)\Pr\left(\left|\hat{h}_{aw}^k\right|^2 \geq \Delta_2\right)\end{aligned} \tag{C.1}$$

Then the four parts of Eq. (C.1) are solved in detail for each of them, which are displayed as follows

$$\Pr\left(\left|\hat{h}_{aw}^k\right|^2 < \Delta_2\right) = \int_0^{\Delta_2} f_{\left|\hat{h}_{aw}^k\right|^2}(x)\,dx, \tag{C.3}$$

$$\begin{aligned}\mathbb{E}\left(\xi^*\left|\left|\hat{h}_{aw}^k\right|\right|^2 \geq \Delta_2\right) &= \int_{\Delta_2}^\infty e^{\frac{(\Lambda_1 - \Lambda_2)x}{\Lambda_1 \beta_{aw}}} f_{\left|\hat{h}_{aw}^k\right|^2}(x)\,dx\\ &= \frac{1}{1 - \beta_{aw}}\int_{\Delta_2}^\infty e^{\frac{(\Lambda_1 - \Lambda_2 - 2\Lambda_1 \beta_{aw} + \Lambda_2 \beta_{aw})x}{\Lambda_1 \beta_{aw}(1 - \beta_{aw})}}\,dx\end{aligned} \tag{C.4}$$

$$\Pr\left(\left|\hat{h}_{aw}^k\right|^2 \geq \Delta_2\right) = 1 - \int_0^{\Delta_2} f_{\left|\hat{h}_{aw}^k\right|^2}(x)\,dx. \tag{C.5}$$

The derivation gives us Eq. (C.2), which you can see at the top of the following page.

The next step is simply to substitute Eqs. (C.2), (C.3), (C.4) and (C.5) into Eq. (19) to obtain the result of **Theorem 3**.

REFERENCES

[1] P. Porambage, G. Gur, D. P. Moya Osorio, M. Livanage, and M. Yliant-tila, "6G security challenges and potential solutions," in *Proc. Jt. Eur. Conf. Networks Commun. 6G Summit (EuCNC/6G Summit)*, Porto, Portugal, Jun. 2021, pp. 622–627.

[2] Q. C. Li, H. Niu, A. T. Papathanassiou, and G. Wu, "5G network capacity: Key elements and technologies," *IEEE Veh. Technol. Mag.*, vol. 9, no. 1, pp. 71–78, Mar. 2014.

[3] Y. Tao, L. Liu, S. Liu, and Z. Zhang, "A survey: Several technologies of non-orthogonal transmission for 5G," *China Commun.*, vol. 12, no. 10, pp. 1–15, Oct. 2015.

[4] Y. Wang, B. Ren, S. Sun, S. Kang, and X. Yue, "Analysis of non-orthogonal multiple access for 5G," *China Commun.*, vol. 13, no. Supplement2, pp. 52–66, 2016.

[5] S. M. R. Islam, N. Avazov, O. A. Dobre, and K.-s. Kwak, "Power-domain non-orthogonal multiple access (NOMA) in 5G systems: Potentials and challenges," *IEEE Commun. Surv. Tutor.*, vol. 19, no. 2, pp. 721–742, Second quarter 2017.

[6] R. Swaroop and A. Kumar, "A brief study and analysis of NOMA techniques for 5G," in *Proc. IEEE Int. Women Eng. Conf. Electr. Comput. Eng. (WIECON-ECE)*, Bhubaneswar, India, Dec. 2020, pp. 13–16.

[7] K. Yang, N. Yang, N. Ye, M. Jia, Z. Gao, and R. Fan, "Non-orthogonal multiple access: Achieving sustainable future radio access," *IEEE Commun. Mag.*, vol. 57, no. 2, pp. 116–121, Feb. 2019.

[8] X. Li, J. Li, Y. Liu, Z. Ding, and A. Nallanathan, "Residual transceiver hardware impairments on cooperative NOMA networks," *IEEE Trans. Wireless Commun.*, vol. 19, no. 1, pp. 680–695, Jan. 2020.

[9] X. Li, H. Liu, G. Li, Y. Liu, M. Zeng, and Z. Ding, "Effective capacity analysis of AmBC-NOMA communication systems," *IEEE Trans. Veh. Technol.*, 2022, doi: 10.1109/TVT.2022.3186871.

[10] X. Li, X. Gao, Y. Liu, G. Huang, M. Zeng, and D. Qiao, "Overlay cognitive radio-assisted NOMA intelligent transportation systems with imperfect SIC and CEEs," *Chin. J. Electron.*, 2022.

[11] Z. Ding, X. Lei, G. K. Karagiannidis, R. Schober, J. Yuan, and V. K. Bhargava, "A survey on non-orthogonal multiple access for 5G networks: Research challenges and future trends," *IEEE J. Sel. Areas Commun.*, vol. 35, no. 10, pp. 2181–2195, Oct. 2017.

[12] Y. Qi and M. Vaezi, "Signaling design for MIMO-NOMA with different security requirements," *IEEE Trans. Signal Process.*, 2022, doi: 10.1109/TSP.2022.3156915.

[13] P. Sindhu, K. Deepak, and K. Abdul Hameed, "A novel low complexity power allocation algorithm for downlink NOMA networks," in *Proc. IEEE Recent Adv. Intell. Comput. Syst. (RAICS)*, Trivandrum, India, Dec. 2018, pp. 36–40.

[14] S. Mounchili and S. Hamouda, "Pairing distance resolution and power control for massive connectivity improvement in NOMA systems," *IEEE Trans. Veh. Technol.*, vol. 69, no. 4, pp. 4093–4103, Apr. 2020.

[15] Z. Xiang, X. Tong, and Y. Cai, "Secure transmission for NOMA systems with imperfect SIC," *China Commun.*, vol. 17, no. 11, pp. 67–78, Nov. 2020.

[16] R. Huang, D. Wan, F. Ji, H. Qing, J. Li, H. Yu, and F. Chen, "Performance analysis of NOMA-based cooperative networks with relay selection," *China Commun.*, vol. 17, no. 11, pp. 111–119, Nov. 2020.

[17] Y. Cai, C. Ke, Y. Ni, J. Zhang, and H. Zhu, "Power allocation for NOMA in D2D relay communications," *China Commun.*, vol. 18, no. 1, pp. 61–69, Jan. 2021.

[18] Y. Cheng, K. H. Li, Y. Liu, and K. C. Teh, "Outage performance of downlink IRS-assisted NOMA systems," in *Proc. IEEE Glob. Commun. Conf. (GLOBECOM)*, Taipei, Taiwan, Dec. 2020, pp. 1–6.

[19] J. Zuo, Y. Liu, Z. Qin, and N. Al-Dhahir, "Resource allocation in intelligent reflecting surface assisted NOMA systems," *IEEE Trans. Commun.*, vol. 68, no. 11, pp. 7170–7183, Nov. 2020.

[20] M. Zeng, X. Li, G. Li, W. Hao, and O. A. Dobre, "Sum rate maximization for IRS-assisted uplink NOMA," *IEEE Commun. Lett.*, vol. 25, no. 1, pp. 234–238, Jan. 2021.

[21] B. A. Bash, D. Goeckel, D. Towsley, and S. Guha, "Hiding information in noise: fundamental limits of covert wireless communication," *IEEE Commun. Mag.*, vol. 53, no. 12, pp. 26–31, Dec. 2015.

[22] A. J. Menzies, P. C. V. Oorschot, and S. A. Vanstone, *Handbook of Applied Cryptography*. Boca Raton, FL, USA: CRC Press, 1996.

[23] X. Li, M. Huang, Y. Liu, V. G. Menon, A. Paul, and Z. Ding, "I/Q imbalance aware nonlinear wireless-powered relaying of B5G networks: Security and reliability analysis," *IEEE Trans. Netw. Sci. Eng.*, vol. 8, no. 4, pp. 2995–3008, Oct.-Dec. 2021.

[24] B. A. Bash, D. Goeckel, and D. Towsley, "Limits of reliable communication with low probability of detection on AWGN channels," *IEEE J. Sel. Areas Commun.*, vol. 31, no. 9, pp. 1921–1930, Sep. 2013.

[25] P. H. Che, M. Bakshi, and S. Jaggi, "Reliable deniable communication: Hiding messages in noise," in *Proc. IEEE Int. Symp. Inf. Theor.*, Istanbul, Turkey, Jul. 2013, pp. 2945–2949.

[26] K. S. K. Arumugam and M. R. Bloch, "Keyless covert communication over multiple-access channels," in *Proc. IEEE Int. Symp. Inf. Theor.*, Barcelona, Spain, Jul. 2016, pp. 2229–2233.

[27] X. Lu, E. Hossain, T. Shafique, S. Feng, H. Jiang, and D. Niyato, "Intelligent reflecting surface enabled covert communications in wireless networks," *IEEE Network*, vol. 34, no. 5, pp. 148–155, Sep./Oct. 2020.

[28] A. Mukherjee, "Physical-layer security in the internet of things: Sensing and communication confidentiality under resource constraints," *Proc. IEEE*, vol. 103, no. 10, pp. 1747–1761, Oct. 2015.

[29] S. Yan, X. Zhou, J. Hu, and S. V. Hanly, "Low probability of detection communication: Opportunities and challenges," *IEEE Wireless Commun.*, vol. 26, no. 5, pp. 19–25, Oct. 2019.

[30] D. Goeckel, B. Bash, S. Guha, and D. Towsley, "Covert communications when the warden does not know the background noise power," *IEEE Commun. Lett.*, vol. 20, no. 2, pp. 236–239, Feb. 2016.

[31] P. H. Che, S. Kadhe, M. Bakshi, C. Chan, S. Jaggi, and A. Sprintson, "Reliable, deniable and hidable communication: A quick survey," in

Proc. IEEE Inf. Theory Workshop, Hobart, TAS, Australia, Nov. 2014, pp. 227–231.

[32] L. Wang, G. W. Wornell, and L. Zheng, "Fundamental limits of communication with low probability of detection," *IEEE Trans. Inf. Theory*, vol. 62, no. 6, pp. 3493–3503, Jun. 2016.

[33] S. Yan, B. He, Y. Cong, and X. Zhou, "Covert communication with finite blocklength in awgn channels," in *Proc. IEEE Int. Conf. Commun. (ICC)*, Paris, France, May 2017, pp. 1–6.

[34] T.-X. Zheng, Z. Yang, C. Wang, Z. Li, J. Yuan, and X. Guan, "Wireless covert communications aided by distributed cooperative jamming over slow fading channels," *IEEE Trans. Wireless Commun.*, vol. 20, no. 11, pp. 7026–7039, Nov. 2021.

[35] L. Yuda, J. Liang, W. Hu, and X. Xiaoming, "Multi-antenna covert communication achieved by exploiting a public communication link," in *Proc. Int. Conf. Wirel. Commun. Signal Process. (WCSP)*, Nanjing, China, Oct. 2020, pp. 883–888.

[36] K. Shahzad, X. Zhou, and S. Yan, "Covert wireless communication in presence of a multi-antenna adversary and delay constraints," *IEEE Trans. Veh. Technol.*, vol. 68, no. 12, pp. 12 432–12 436, Dec. 2019.

[37] C. Gao, B. Yang, X. Jiang, H. Inamura, and M. Fukushi, "Covert communication in relay-assisted IoT systems," *IEEE Internet Things J.*, vol. 8, no. 8, pp. 6313–6323, Apr. 2021.

[38] M. Forouzesh, P. Azmi, A. Kuhestani, and P. L. Yeoh, "Covert communication and secure transmission over untrusted relaying networks in the presence of multiple wardens," *IEEE Trans. Commun.*, vol. 68, no. 6, pp. 3737–3749, Jun. 2020.

[39] B. He, S. Yan, X. Zhou, and H. Jafarkhani, "Covert wireless communication with a poisson field of interferers," *IEEE Trans. Wireless Commun.*, vol. 17, no. 9, pp. 6005–6017, Sep. 2018.

[40] O. A. Topal and G. K. Kurt, "Covert communication in cooperative NOMA networks," in *Proc. 28th Signal Process. Commun. Appl. Conf. (SIU)*, Gaziantep, Turkey, Oct. 2020, pp. 1–4.

[41] H. Peng, W. He, Y. Zhang, X. Li, Y. Ding, V. G. Menon, and S. Verma, "Covert non-orthogonal multiple access communication assisted by multi-antenna jamming," *Phys. Commun.*, vol. 52, p. 101598, Jan. 2022.

[42] L. Tao, W. Yang, X. Lu, M. Wang, and Y. Song, "Achieving covert communication in uplink NOMA systems via energy harvesting jammer," *IEEE Commun. Lett.*, vol. 25, no. 12, pp. 3785–3789, Dec. 2021.

[43] M. Wang, W. Yang, X. Lu, C. Hu, B. Liu, and X. Lv, "Channel inversion power control aided covert communications in uplink NOMA systems," *IEEE Wireless Commun. Lett.*, vol. 11, no. 4, pp. 871–875, Apr. 2022.

[44] L. Lv, Q. Wu, Z. Li, Z. Ding, N. Al-Dhahir, and J. Chen, "Achieving covert communication by IRS-NOMA," in *Proc. IEEE/CIC Int. Conf. Commun. China (ICCC)*, Xiamen, China, Jul. 2021, pp. 421–426.

[45] K. Shahzad, X. Zhou, and S. Yan, "Covert communication in fading channels under channel uncertainty," in *Proc. IEEE 85th Veh. Technol. Conf. (VTC Spring)*, Sydney, NSW, Australia, Jun. 2017, pp. 1–5.

[46] L. Tao, W. Yang, S. Yan, D. Wu, X. Guan, and D. Chen, "Covert communication in downlink noma systems with random transmit power," *IEEE Wireless Commun. Lett.*, vol. 9, 2020.

[47] A. K. Gurung, F. S. Al-Qahtani, Z. M. Hussain, and H. Alnuweiri, "General order antenna selection in dual-hop amplify forward system with multi-antenna relay," in *Proc. Int. Conf. Adv. Technol. Commun.*, Ho Chi Minh City, Vietnam, Oct. 2010, pp. 311–315.

[48] B. He and X. Zhou, "Secure on-off transmission design with channel estimation errors," *IEEE Trans. Inf. Forensics Secur.*, vol. 8, no. 12, pp. 1923–1936, Dec. 2013.

[49] A. Vakili, M. Sharif, and B. Hassibi, "The effect of channel estimation error on the throughput of broadcast channels," in *Proc. IEEE Int. Conf. Acoust. Speech Signal Process.*, vol. 4, Toulouse, France, May 2006, pp. IV–IV.

[50] B. C. Levy, *Principles of Signal Detection and Parameter Estimation*. New York: Springer, 2010.

[51] T. V. Sobers, B. A. Bash, S. Guha, D. Towsley, and D. Goeckel, "Covert communication in the presence of an uninformed jammer," *IEEE Trans. Wireless Commun.*, vol. 16, no. 9, pp. 6193–6206, Sep. 2017.